Monocular Camera Calibration based on Genetic Simulated Annealing Algorithms

Hafsa Khrouch
IEVIA team, IMAGE Laboratory, ESTM, Moulay Ismail University of Meknes, Morocco
h.khrouch@edu.umi.ac.ma (corresponding author)

Abdelaaziz Mahdaoui
IEVIA team, IMAGE Laboratory, ESTM, Moulay Ismail University of Meknes, Morocco
a.mahdaoui@edu.umi.ac.ma

Mostafa Merras
IEVIA team, IMAGE Laboratory, ESTM, Moulay Ismail University of Meknes, Morocco
m.merras@umi.ac.ma

Abdellah Marhraoui Hsaini
IEVIA team, IMAGE Laboratory, ESTM, Moulay Ismail University of Meknes, Morocco
mhabdallah@gmx.fr

Idriss Chana
SCIAM team, IMAGE Laboratory, ESTM, Moulay Ismail University of Meknes, Morocco
idrisschana@gmail.com

Aziz Bouazi
IEVIA team, IMAGE Laboratory, ESTM, Moulay Ismail University of Meknes, Morocco
a.bouazi@gmx.fr

Received: 12 August 2024 | Revised: 20 September 2024 | Accepted: 6 October 2024

 DOI: https://doi.org/10.48084/etasr.8710

ABSTRACT

This study presents a nonlinear camera calibration approach based on combining genetic and simulated annealing algorithms. This is a global optimization technique, which combines simulated annealing with genetic algorithms to find the optimal camera's intrinsic and extrinsic parameters. Since this matter is considered an optimization problem by several studies, a novel hybrid approach was developed and studied based on two powerful nature-inspired techniques to find the intrinsic and extrinsic parameters of the camera. Numerous experiments were conducted to evaluate the efficiency of the proposed approach. The results demonstrate that the proposed hybrid approach is robust, reliable, and accurate.

Keywords-camera calibration; genetic algorithm; simulated annealing; optimization; fitness function; radial distortion

I. INTRODUCTION

The camera calibration process in 3D image processing and graphics refers to modeling the image formation operation, that is, determining the connection between the spatial coordinates of a point and its corresponding position in the camera image [1-6]. The geometric calibration of a camera involves identifying the mathematical relationship that exists between the 3D coordinates of the points of the scene and the 2D coordinates of their projection in the image. 3D reconstruction [7-8], recognition, object localization, dimensional control of parts, and environmental reconstruction for mobile robot navigation are applications of artificial vision that begin with the camera calibration stage.

Different camera calibration methods exist, which fall into two categories, analytical techniques and those based on metaheuristic algorithms [9]. This study falls into the second group based on metaheuristic algorithms. This type formulates camera calibration as a problem of optimizing a cost function. This article focuses on methods that use the Genetic Algorithm

(GA) [10-11] and the Simulated Annealing algorithm (SA) [12]. GA belongs to the category of evolutionary algorithms, as they are auto-adaptive stochastic search methods [10]. A GA creates new people using selection, crossover, and mutation operators. It is a global search technique that has been effectively used to solve a variety of situations. SA is a probabilistic metaheuristic used to approximate global optimization in large search spaces, particularly in discrete environments [12]. It is effective in finding global optima among numerous local optima and can outperform methods such as gradient descent when estimating a global solution is more important than finding an exact local one. SA, inspired by the natural annealing process in metals, is widely used for its ability to escape local minima.

GA-SA, or genetic algorithm-simulated annealing, is a hybrid algorithm that combines the best features of both GA and SA to offer a novel fast global optimization search method. The neighborhood structure in the search process can be enhanced by the GA-SA, which also enhances the range of values that can be searched. This study discusses the problem of nonlinear camera calibration and formulates it as an optimization problem. For this purpose, a combined Genetic Algorithm Simulated Annealing (GASA) algorithm was developed. By improving the results of the camera parameters, this method seeks to reduce the reprojection error. In the context of camera calibration, it is also demonstrated how the integration of distortions influences the cost function by comparing the camera calibration with and without distortion. Furthermore, GASA was compared to other existing methods. The acquisition of a reliable assessment of the extrinsic and intrinsic parameters of the camera was made possible by the ability of the proposed technique to converge quickly to an ideal result and avoid local minima. This study presents several important contributions to the field of camera calibration. The main contributions are as follows:

- The proposed method can be applied to the calibration problem regardless of the camera model (i.e., whether the camera model has distortions or not).
- Only an image of the target is needed to estimate the camera parameters.
- The combination of the two algorithms takes advantage of the complementary strengths of each method to offer a more efficient optimization. The GA widely explores the solution space by generating a diversity of candidates, while the SA refines these solutions by avoiding local minima and converging to more precise optima. This combination improves the quality of the solutions and accelerates convergence.

II. BACKGROUND

A. Camera Model

Camera calibration involves developing equations that describe the relationship between the 3D coordinates of known feature points and their corresponding 2D coordinates in an image. By solving these equations, intrinsic and extrinsic camera parameters are obtained. Figure 1 shows the frequently used pinhole model

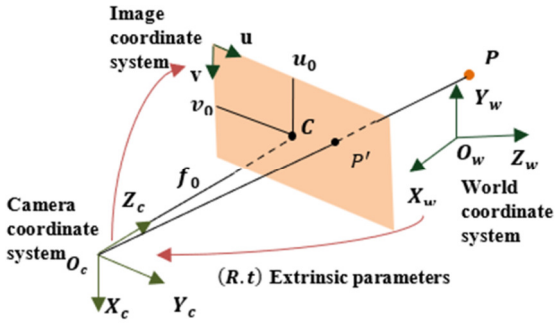

Fig. 1. The pinhole imaging model.

$O_w - X_w, Y_w, Z_w$ is the world coordinate system, $O - u, v$ is the image coordinate system, and $O_c - X_c, Y_c, Z_c$ is the camera coordinate system. In line with this model, the following formula can be used to convert a point P in the world coordinate system to the pixel coordinate system P':

$$P' \sim M_i M_e P \tag{1}$$

Intrinsic parameters describe the camera's optical and geometrical properties, including the center of the image represented by (u_0, v_0) (principal point), and the effective size of pixels represented by (α_u, α_v). The mathematical representation of the camera's intrinsic parameters is given by the following matrix:

$$M_i = \begin{bmatrix} \alpha_u & 0 & u_0 & 0 \\ 0 & \alpha_v & v_0 & 0 \\ 0 & 0 & 1 & 0 \end{bmatrix} \tag{2}$$

where $\alpha_u = f_0 K_u$, $\alpha_v = f_0 K_v$, f_0 is the focal length, and K_u and K_v represent the scaling factors. Regarding the extrinsic matrix M_e, the transformation from 3D world coordinates to camera coordinates is defined by a rotation matrix R, and a three-element translation vector, T, as follows:

$$M_e = \begin{bmatrix} r_{11} & r_{12} & r_{13} \\ r_{21} & r_{22} & r_{23} \\ r_{31} & r_{32} & r_{33} \end{bmatrix} . \begin{bmatrix} t_x \\ t_y \\ t_z \end{bmatrix} \tag{3}$$

Using (2) and (3), the transformation matrix M can be reformulated as:

$$M = \begin{bmatrix} \alpha_u & 0 & u_0 & 0 \\ 0 & \alpha_v & v_0 & 0 \\ 0 & 0 & 1 & 0 \end{bmatrix} . \begin{bmatrix} r_{11} & r_{12} & r_{13} \\ r_{21} & r_{22} & r_{23} \\ r_{31} & r_{32} & r_{33} \end{bmatrix} . \begin{bmatrix} t_x \\ t_y \\ t_z \end{bmatrix} \tag{4}$$

The following equation can be deduced:

$$\begin{bmatrix} s_u \\ s_v \\ s \end{bmatrix} = \begin{bmatrix} \alpha_u & 0 & u_0 & 0 \\ 0 & \alpha_v & v_0 & 0 \\ 0 & 0 & 1 & 0 \end{bmatrix} . \begin{bmatrix} r_{11} & r_{12} & r_{13} & t_x \\ r_{21} & r_{22} & r_{23} & t_y \\ r_{31} & r_{32} & r_{33} & t_z \\ 0 & 0 & 0 & 1 \end{bmatrix} . \begin{bmatrix} X_w \\ Y_w \\ Z_w \\ 1 \end{bmatrix} \tag{5}$$

and the following equation can be obtained [13]:

$$\begin{cases} u = \alpha_u \frac{r_{11} P_{Xw} + r_{12} P_{Yw} + r_{13} P_{Zw} + t_x}{r_{31} P_{Xw} + r_{32} P_{Yw} + r_{33} P_{Zw} + t_z} + u_0 \\ v = \alpha_v \frac{r_{21} P_{Xw} + r_{22} P_{Yw} + r_{23} P_{Zw} + t_y}{r_{31} P_{Xw} + r_{32} P_{Yw} + r_{33} P_{Zw} + t_z} + v_0 \end{cases} \tag{6}$$

The relationship between an object's 3D coordinates and their corresponding 2D coordinates on an image is described by

the condition of collinearity, which ensures that the camera's projection center, the object's points, and the image's points are all oriented on the right.

B. Genetic Algorithm

GA [10] is part of evolutionary algorithms and aims to approximate solutions to optimization models and search problems. It is a bioinspired optimization approach that replicates evolutionary processes by randomly selecting new individuals from the current population each time. Figure 2 presents the flowchart of the GA.

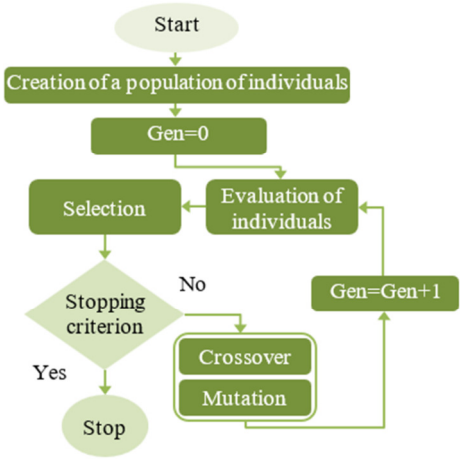

Fig. 2. Flowchart of GA.

The application of these genetic principles uses three fundamental evolution operators:

- Selection: This involves choosing the most suitable individuals from the population based on their adaptation to the problem.
- Crossover: Combining traits from selected individuals to create new solutions.
- Mutation: Introduces random changes to an individual's traits to explore new potential solutions.

By leveraging these principles and operators, GAs iteratively evolve populations of solutions toward increasingly optimal approximations of the problem's solution.

C. Simulated Annealing

SA [12] is a probabilistic optimization algorithm inspired by the annealing process in metallurgy, where materials are heated and then cooled slowly to eliminate defects and reduce the strength of the process. It is easy to implement and applies to various optimization problems. However, it can be resource-intensive due to the high number of iterations required, and its efficiency strongly depends on the chosen parameters and cooling schedule. The main considerations are explained as follows.

- Initial State s_0: The starting point of the algorithm.
- Energy Function $f(s)$: A function that evaluates the cost or quality of a solution s.
- Neighbor Function $N(s)$: A function that generates a neighboring solution s' from the current solution s.
- Temperature T: A parameter that controls the probability of accepting worse solutions. It decreases over time according to the cooling schedule.
- Cooling Schedule $T_k = \rho \cdot T_k - 1$: A function that reduces the temperature T over time, typically a geometric decay where ρ is between 0 and 1.
- Acceptance Probability: If the new solution s' has a lower energy, it is always accepted. If s' has a higher energy, it is accepted with a probability $exp^{(-\frac{\Delta f}{T})}$, where Δf is the difference in energy between s' and s.

The SA algorithm is described as follows.

```
Algorithm1: Simulated Annealing (SA)
T← T0 // T0 is the temperature initialized
// at a large value.
s ← s0 ; s0 is an initial solution.
Best ← s;
While (s = Best && T ≤ max && T ≥ 0) do
  r ← s' where s'∈ N(s) // N(s) Indicates
  // the neighbors of a solution S.
  ρ ← random (0,1)
  if (f(r) < f(s) or ρ < e^(-(f(r) - f(s))/T)) then
   s ← r
  endif
  if (f(s) < f(best)) then
   best ← s
  endif
  decrease T ← ρT
EndWhile
```

D. Related Works

There are certain applications for the hybrid algorithm [14], in image processing. In [15], the aim was to distinguish ice-covered cables from their background in low-contrast images, which are crucial to monitoring power lines under snow. A method was proposed that combined the 2D Otsu algorithm with a simulated annealing genetic algorithm, optimized for more accurate segmentation and faster search. In [16], an innovative hybrid technique was proposed, which combined GA with SA to optimize Fractal Image Compression (FIC). This technique sought to reduce the complexity of searching for range and domain block matching while decreasing the high computational time often associated with FIC.

1) Analytical Methods

The analytical method using linear perspective projection extracts intrinsic and extrinsic parameters but lacks precision and robustness. In [17], an adaptable method was proposed for rapid camera calibration using a planar pattern viewed in at least two different orientations. This approach combined a closed-form solution with nonlinear refinement based on maximum likelihood criteria. In [18], a novel method was proposed for 3D camera calibration using standard TV cameras

and lenses. This approach computed the camera's position and orientation first, followed by internal parameters such as focal length and radial lens distortion, ensuring efficient calibration relative to the object reference system. In [19], a four-step calibration process was presented. One step was used for fixing the distorted picture coordinates and another to account for distortion brought on by circular features. An empirical inverse model was used for image rectification to address tangential and radial distortions, with parameters determined through a linear approach.

2) Metaheuristic Algorithm-based Techniques

In [20], the standard genetic algorithm's encoding technique was improved by using an adaptive adjustment function of variable intervals. An improved genetic procedure can ensure sufficient encoding precision while maintaining an appropriate search space. In [21], the Particle Swarm Optimisation (PSO) algorithm was used to determine the intrinsic characteristics of the camera. In [22], a new approach was proposed for concurrently determining 19 RGB and depth camera calibration parameters. Deep optimization can use metaheuristic techniques, including GA, PSO, Colonial Competitive Algorithm (CCA), and Shuffled Frog Leaping Algorithm (SFLA) to estimate all intrinsic, extrinsic, and lens distortion parameters of cameras.

Other studies proposed a complete GASA-based camera calibration method to combine the benefits of SA and GA. In [23], a complete GASA-based camera elaboration method was proposed that combined the benefits of a simulated circuit and a GA. This algorithm was applied to optimize the camera elaboration results. In [24], an enhanced adaptive genetic SA approach based on the sigmoid function was developed to increase the accuracy of camera calibration, with a focus on the camera imaging problem of the stereo vision system of a marine unmanned ship. In [25], a method for camera calibration was proposed using a hybrid neural network with a rotational weight matrix and a self-adaptive GA algorithm. Two types of structured neural networks estimated the extrinsic and intrinsic parameters of the camera, accounting for both radial distortion and no distortion. Performance was evaluated using the 2-norm of the difference between projected retinal coordinates and network outputs. The GA adjusted the crossover and mutation probabilities, refining the camera parameters with radial distortion as the system approached equilibrium.

III. PROPOSED METHOD

In this study, the camera calibration problem involves the optimization of intrinsic and extrinsic parameters of the camera. This requires the use of algorithms that are capable of efficiently exploring the search space. For this reason, a hybrid approach was developed by combining GA and SA. GA is capable of performing a global search in large and complex solution spaces. It uses mechanisms such as crossover and mutation to avoid local minima and maintain a diverse set of solutions, thus improving exploration. Moreover, GA can be applied to a wide range of optimization problems without requiring detailed prior knowledge of the problem. SA is another powerful optimization technique known for its efficiency in exploring complex solution spaces. It is particularly adept at avoiding local minima by using a probabilistic approach that allows occasional acceptance of worse solutions, which can help escape local optima. GA enables a rapid and diverse exploration of the solution space, while SA refines this exploration.

A. Problem Formulation

Radial distortions are the most common kind caused by camera lenses. They are typically taken into account by the computer vision scientific community, notably with the work of [18]. These distortions use the image coordinates of the optical axis center as a reference point, creating a non-linear relationship with the distance from this reference point to any image point. To achieve high-accuracy calibration, it is essential to consider and model lens distortion. The correction made to a point (u, v), expressed in a frame whose origin coincides with the center of the radial distortions, is carried out by moving this point by a vector defined by:

$$\begin{cases} \Delta u_R = \tilde{u}\ (k_1 r^2 + k_2 r^4 + \cdots) = \tilde{u} \sum_{i=1}^{n} k_1 r^{2i} \\ \Delta v_R = \tilde{v}\ (k_1 r^2 + k_2 r^4 + \cdots) = \tilde{v} \sum_{i=1}^{n} k_1 r^{2i} \end{cases} \quad (7)$$

with:

$$\tilde{u} = (u - u_0) \quad (8)$$

$$\tilde{v} = (u - v_0) \quad (9)$$

$$r = \sqrt{u^2 + v^2} \quad (10)$$

The use of a single radial distortion coefficient, which is frequently mentioned as k_1, is an easy and effective method to calibrate cameras. This coefficient is used to correct radial distortion that deforms objects at the periphery of the camera. By focusing on this single parameter, the main distortion can be addressed while keeping the model simple, making it suitable for many applications. For first-degree radial distortion, the following model is obtained [13]:

$$\begin{cases} u = \alpha_u \frac{r_{11} P_{XW} + r_{12} P_{YW} + r_{13} P_{ZW} + t_x}{r_{31} P_{XW} + r_{32} P_{YW} + r_{33} P_{ZW} + t_z} + u_0 + k_1 \tilde{u} r^2 \\ v = \alpha_v \frac{r_{21} P_{XW} + r_{22} P_{YW} + r_{23} P_{ZW} + t_y}{r_{31} P_{XW} + r_{32} P_{YW} + r_{33} P_{ZW} + t_z} + v_0 + k_1 \tilde{v} r^2 \end{cases} \quad (11)$$

B. Estimation of Camera Parameters by GASA

This section presents a GASA algorithm that brings together two metaheuristic algorithms, GA and SA, for the estimation of camera parameters. The process of estimation involves the minimization of a non-linear cost function that calculates the Euclidean distance between the estimated and real 2D points. The GA and SA stages of GASA are shown in Figure 3. First, GA produces the starting population randomly using the enhanced hybrid method. After assessing the original population, GA applies three genetic operators to the population to generate a new population. The top individual is sent by GA to SA for additional development after every generation. Once the individual has completed their further development, SA transfers it to GA for the following generation. This procedure keeps going until the algorithm's termination condition is satisfied. Based on Figure 3, a detailed description of some components related to the two stages is provided below.

1) Phase I: The GA Optimal Process

The first population is generated randomly by GA, which then applies three genetic operators to the population to create a new one. Figure 2 suggests that certain elements related to GA should be ascertained, including population size, initial population generation, population evaluation, chromosomal encoding, genetic operators (selection, crossover, mutation), and termination condition. Vector b contains the camera parameters to be optimized:

$$b = \left[u_0, v_0, \alpha_u, \alpha_v, t_x, t_y, t_z, \alpha, \beta, \gamma, k_1 \right] \quad (12)$$

The vector b is denoted as $b = (b_1, b_2, \ldots\ldots, b_i)$, where b_i represents the previously defined parameters. This vector represents a potential solution to the camera calibration problem and belongs to the established possible solutions B such that $B = \{b : b_i \in [b_i^-, b_i^+]; i = 1,2, \ldots, n\}$, where the limits of the variation interval for each parameter are denoted by b_i^- and b_i^+. The bounds of each interval are derived from our knowledge of the camera, then these bounds are provided to the GA as input. For unknown parameters, large bounds can be established. The fitness function given by (13) is minimized to find the optimal solution for b. Table I shows the range of variation for the camera parameters.

TABLE I. VARIATION INTERVALS FOR THE CAMERA'S PARAMETERS

Notation	Bounds (b_i^-, b_i^+)	Unit
u_0	[1900,2100]	Pixel
v_0	[1400,1600]	Pixel
α_u	[2800,3100]	Pixel
α_v	[2800,3100]	Pixel
α	$[-\pi, \pi]$	Radian
β	$[-\pi, \pi]$	Radian
γ	$[-\pi, \pi]$	Radian
t_x	[−400,400]	mm
t_y	[−400,400]	mm
t_z	[600,1000]	mm
k_1	[−0.5,0.5]	-

The primary objective of this approach is to determine the intrinsic and extrinsic parameters that give the minimum reprojection error using the following cost function:

$$f(w) = \sum_{i=1}^{P} [(d(w, X_i) - u_i)^2 + (e(w, X_i) - v_i)^2] \quad (13)$$

where P is the number of control points, (u_i, v_i) are 2D real coordinates, and $d(w, X_i)$ and $e(w, X_i)$ are the 2D estimated coordinates, with $i = 1, \ldots, N$.

$$\begin{cases} d(w, X_i) = \alpha_u \frac{r_{11}P_{Xw} + r_{12}P_{Yw} + r_{13}P_{Zw} + t_x}{r_{31}P_{Xw} + r_{32}P_{Yw} + r_{33}P_{Zw} + t_z} + u_0 + k_1 \tilde{u}_i r^2 \\ e(w, X_i) = \alpha_v \frac{r_{21}P_{Xw} + r_{22}P_{Yw} + r_{23}P_{Zw} + t_y}{r_{31}P_{Xw} + r_{32}P_{Yw} + r_{33}P_{Zw} + t_z} + v_0 + k_1 \tilde{v}_i r^2 \end{cases} \quad (14)$$

2) Phase II: The SA's Optimal Process

The GA will forward its top individual to the SA. The SA transfers the best individual to the GA for the following generation after the GA has enhanced it. This procedure continues until the algorithm's termination condition is satisfied. The objective function of SA and GA should be merged to minimize the SA objective function. This approach maximizes the efficiency of each method and is more effective than a nested approach. Certain aspects of the SA algorithm should be taken into account when analyzing Figure 3. These include selecting the starting temperature, the pace at which the temperature decreases as cooling occurs, the number of switches at each temperature, and the procedure's termination. These elements are crucial to the SA's operation and have to be completed with attention. Figure 3 presents the flowchart of the proposed method:

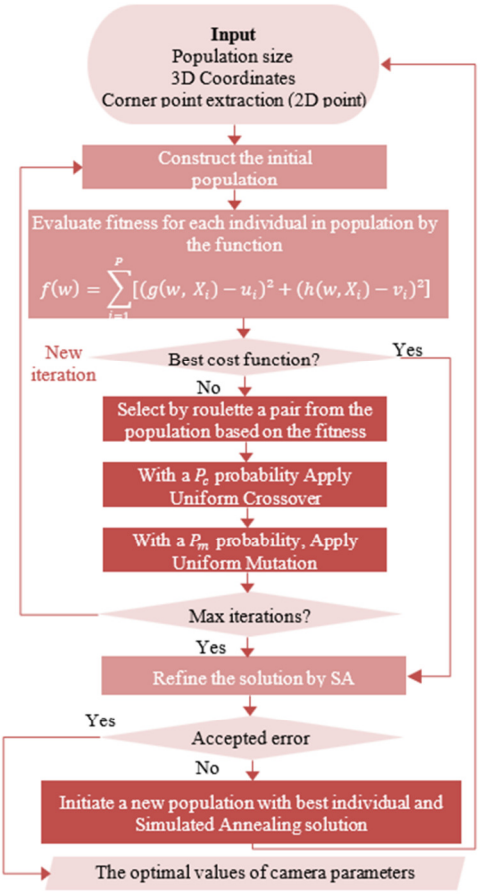

Fig. 3. Flowchart of the proposed method.

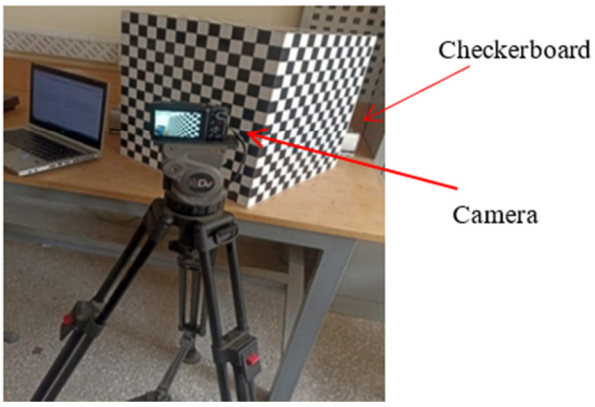

Fig. 4. The experimental setup.

IV. EXPERIMENTAL RESULTS AND DISCUSSION

This section presents experiments on real images to demonstrate the effectiveness of the proposed approach. As shown in Figure 4, the experimental system consists of a 3D calibration target with 30×30 mm squares and a CCD camera with a resolution of 4000×3000 pixels. Table II presents GASA parameters.

TABLE II. PARAMETERS OF GASA

Parameter	Value
Population size	500
Crossover probability	0.7
Crossover type	Uniform
Mutation probability	0.1
Mutation type	Uniform
Selection type	Linear-Ranking
Temperature	1000
Step size	0.01
Number of iterations	10000

A. Accuracy of the Proposed Method

The proposed method aims to minimize the cost function, which is crucial as it provides a quantitative measure of the calibration's accuracy. By minimizing the cost function, it is ensured that the estimated camera parameters produce projections that closely match the observed image points. Figure 5 presents the evolution of the fitness function. Applying the optimization model results in three development phases aiming at maximizing population performance. The first phase involves an initial period of rapid development. The second phase indicates a slowdown in evolution. The third phase reveals a stagnation in the cost function. Therefore, it can be concluded that GASA converges effectively. Table III shows the camera parameters estimated by GASA under undistorted and distorted conditions.

The 2D coordinates (u', v') of the camera parameters are derived from the transformation relationship between the camera calibration model and the 3D spatial coordinates (X^w, Y^w, Z^w). Then, they are compared with the real image coordinate (u, v) obtained by applying the Canny filter [26], making it possible to validate the precision and dependability of the camera calibration approach. Tables IV and V show the real and estimated values of the 2D coordinates of the obtained corner under undistorted and distorted conditions, respectively. The coordinates u' and v' represent the estimated 2D coordinates, although u and v denote the real 2D coordinates.

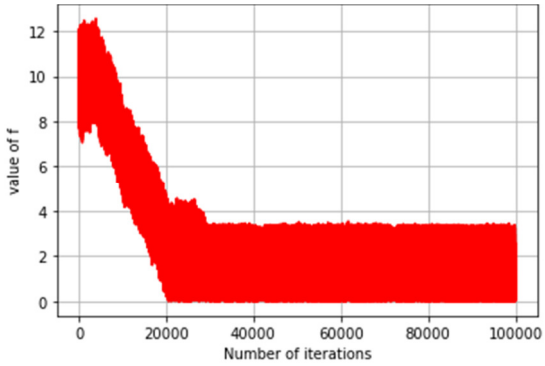

Fig. 5. Evolution of the fitness function of GASA.

TABLE III. COMPARISON OF CAMERA PARAMETERS UNDER UNDISTORTED AND DISTORTED CONDITIONS

Parameter	Value (GASA undistorted conditions)	Value (GASA distorted conditions)
u_0 (Pixel)	$1.92420.10^3$	$1.92173.10^3$
v_0 (Pixel)	$1.42683.10^3$	$1.42838.10^3$
α_u (Pixel)	$3.04859.10^3$	$3.04414.10^3$
α_v (Pixel)	$3.04336.10^3$	$\mathbf{3.04210.10^3}$
t_x (mm)	$7.278.10^1$	$7.165.10^1$
t_y (mm)	$-1.8641.10^2$	$-1.8676.10^2$
t_z (mm)	$8.9475.10^2$	$8.9116.10^2$
α (Radian)	$4.3.10^{-3}$	$4.3.10^{-3}$
β (Radian)	$-8.3.10^{-1}$	$-8.0.10^{-1}$
γ (Radian)	$3.19.10^{-2}$	$3.0.10^{-2}$
k_1	0	$1.1.10^{-9}$

TABLE IV. RELIABILITY VERIFICATION RESULTS OF GASA (UNDISTORTED CONDITIONS)

$x(mm)$	$y(mm)$	$z(mm)$	$u\ (pixels)$	$u'\ (pixels)$	$\lvert u-u'\rvert$	$v\ (pixels)$	$v'\ (pixels)$	$\lvert v-v'\rvert$
90	180	0	2334.085	2327.301	6.784	1412.470	1412.338	0.132
90	240	0	2328.046	2320.542	7.504	1604.887	1602.064	2.823
150	240	0	2439.601	2431.729	7.872	1600.015	1598.271	1.744
0	270	90	1914.385	1915.955	1.570	1687.584	1684.328	3.256
0	120	150	1800.149	1795.537	4.612	1211.735	1210.964	0.771
0	120	60	2002.865	2003.436	0.571	1203.503	1205.119	1.616
30	90	0	2196.229	2197.015	0.786	1911.211	1911.397	0.186

TABLE V. RELIABILITY VERIFICATION RESULTS OF GASA (DISTORTED CONDITIONS)

$x(mm)$	$y(mm)$	$z(mm)$	$u\ (pixels)$	$u'\ (pixels)$	$\lvert u-u'\rvert$	$v\ (pixels)$	$v'\ (pixels)$	$\lvert v-v'\rvert$
90	180	0	2334.085	2333.734	0.351	1412.470	1412.387	0.083
90	240	0	2328.046	2327.530	0.516	1604.887	1604.787	0.100
150	240	0	2439.601	2438.720	0.881	1600.015	1601.136	1.121
0	270	90	1915.954	1915.955	0.001	1687.584	1687.568	0.016
0	120	150	1800.149	1799.305	0.844	1211.735	1211.306	0.429
0	120	60	2002.865	2002.679	0.186	1203.503	1204.150	0.647
30	90	0	2196.229	2196.000	0.229	1911.211	1911.197	0.014

As shown in Tables IV and V, after incorporating distortions into the calibration process, the results show improved accuracy. Integrating distortion parameters into the camera calibration model significantly enhances the precision of projecting 3D points onto the image. By including these parameters, the model adjusts the projected coordinates to compensate for lens-induced distortions, thereby minimizing deviations between the projections and the actual point locations.

B. Comparison with Other Methods

To evaluate the precision and performance of the proposed method, eight images of 4000×3000 pixels of a 3D checkerboard were simulated. This target was projected onto the images from various viewpoints using a CCD camera. The reprojection error was then computed after estimating the camera parameters using the proposed method. For comparison, the methods in [18], [17], and [3] were also implemented. Relative error is a crucial indicator for evaluating the performance of an algorithm, particularly when it comes to quantifying the gap between the values calculated by the algorithm and the reference values. In this study, it was calculated for intrinsic parameters (α_u, α_v, u_0 and v_0). The results shown in Figure 6, indicate that the proposed method exhibits a significantly lower relative error compared to the other approaches. This low relative error rate attests to the robustness and precision of the proposed algorithm, indicating that it can reproduce the parameters with high accuracy relative to the reference values. These results confirm the effectiveness of the proposed approach in solving the camera calibration problem.

As part of the performance evaluation of the proposed method, the reprojection error was calculated for 2D points. This error was determined by measuring the difference between the coordinates of the points projected by the calibrated model and the coordinates of the points observed in the images. To make a proper comparison, the errors obtained with the proposed method were compared with those obtained using [18], [17], and [3].

TABLE VI. REPROJECTION ERRORS COMPARISON

	Proposed method	**[3]**	**[17]**	**[18]**
Reprojection error	0.55	0.60	0.71	0.83

Table VI shows that the reprojection errors of the proposed method are considerably reduced compared to those of [18], [17], and [3]. The results demonstrate that the proposed approach is more efficient than the other methods. A key advantage of the proposed method is its flexibility, as it can be applied to any vision system or camera, ensuring a more robust calibration process without system-specific constraints. Furthermore, only a single target image is required to estimate the camera parameters. The use of the GASA algorithm further optimizes the results.

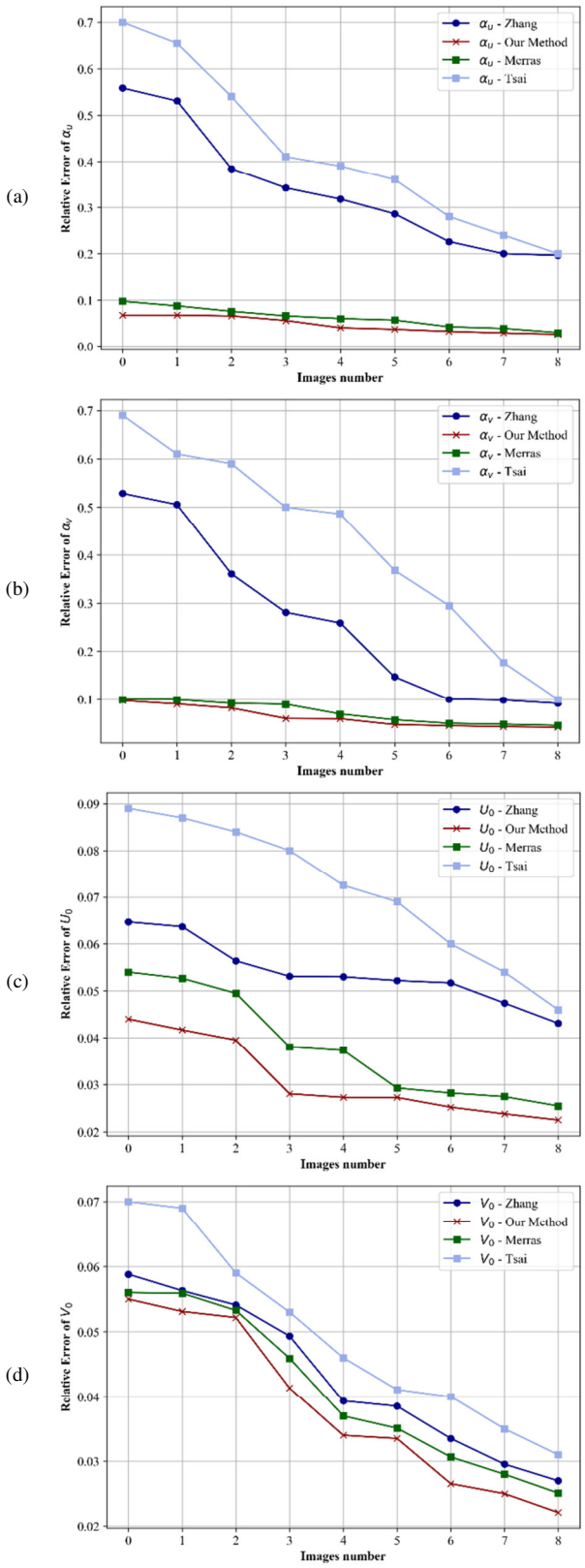

Fig. 6. Results of camera calibration using the proposed approach, Zhang [17], Tsai [18], and Merras [3]: (a) Relative error of α_u, (b) Relative error of α_v, (c) Relative error of u_0 , (d) Relative error of v_0.

Techniques that use metaheuristic optimization algorithms, such as the one in [3], generally offer higher precision and reliability compared to traditional methods. The method in [17], which uses the Levenberg-Marquardt algorithm, requires an initial solution to be sufficiently close to the optimal solution to ensure effective convergence. Regarding the method in [18], it is typically less accurate than the method in [17]. In contrast, the proposed method is more precise than the one in [3] because it combines the strengths of GA and SA. This combination leverages the global search capabilities of GA while incorporating the local adjustments provided by SA, enhancing the robustness and effectiveness of the results.

V. CONCLUSION

This study presented a combined optimization approach applied to camera calibration aimed at determining optimal parameters. The GASA method helps avoid local optima and overcomes the premature convergence of GA. The results show that GASA is a promising technique to address complex camera calibration optimization problems, improving both precision and robustness. This approach surpasses the limitations of existing methods by optimizing distortion control, using only a single image regardless of the camera type or vision system, and leveraging the strengths of both algorithms for better convergence. Although this method takes longer to compute, it offers a robust solution for estimating camera parameters. To improve computation time, the GASA algorithm can be enhanced by dynamically adjusting parameters such as mutation rate, step size, and simulated annealing temperature.

REFERENCES

[1] H. Khrouch, A. M. Hsaini, A. Bouazi, and I. Chana, "Experimental camera calibration study for 3D localisation," in *2022 2nd International Conference on Innovative Research in Applied Science, Engineering and Technology (IRASET)*, Meknes, Morocco, Mar. 2022, pp. 1–4, https://doi.org/10.1109/IRASET52964.2022.9738066.

[2] H. Khrouch, A. Mahdaoui, M. Tantaoui, I. Chana, and A. Bouazi, "Camera Calibration Based on Elitist Genetic Algorithm," in *2024 4th International Conference on Innovative Research in Applied Science, Engineering and Technology (IRASET)*, FEZ, Morocco, May 2024, pp. 1–7, https://doi.org/10.1109/IRASET60544.2024.10549372.

[3] M. Merras, N. E. Akkad, A. Saaidi, G. Nazih, and K. Satori, "Camera Calibration with Varying Parameters Based On Improved Genetic Algorithm," *WSEAS Transactions on Computers*, vol. 13, pp. 129–137, 2014.

[4] M. Merras, N. E. Akkad, A. Saaidi, A. G. Nazih, and K. Satori, "Camera Self Calibration with Varying Parameters by an Unknown Three Dimensional Scene Using the Improved Genetic Algorithm," *3D Research*, vol. 6, no. 1, Feb. 2015, Art. no. 7, https://doi.org/10.1007/s13319-015-0039-6.

[5] S. El Hazzat, N. El Akkad, M. Merras, A. Saaidi, and K. Satori, "Fast 3D reconstruction and modeling method based on the good choice of image pairs for modified match propagation," *Multimedia Tools and Applications*, vol. 79, no. 11, pp. 7159–7173, Mar. 2020, https://doi.org/10.1007/s11042-019-08379-2.

[6] A. Mahdaoui and E. H. Sbai, "3D Point Cloud Simplification Based on k-Nearest Neighbor and Clustering," *Advances in Multimedia*, vol. 2020, no. 1, 2020, Art. no. 8825205, https://doi.org/10.1155/2020/8825205.

[7] S. El Hazzat and M. Merras, "Improvement of 3D reconstruction based on a new 3D point cloud filtering algorithm," *Signal, Image and Video Processing*, vol. 17, no. 5, pp. 2573–2582, Jul. 2023, https://doi.org/10.1007/s11760-022-02474-y.

[8] M. Merras, S. El Hazzat, A. Saaidi, K. Satori, and A. G. Nazih, "3D face reconstruction using images from cameras with varying parameters," *International Journal of Automation and Computing*, vol. 14, no. 6, pp. 661–671, Dec. 2017, https://doi.org/10.1007/s11633-016-0999-x.

[9] M. Merras, N. El Akkad, A. Saaidi, A. Gadhi Nazih, and K. Satori, "A new method of camera self-calibration with varying intrinsic parameters using an improved genetic algorithm," in *2013 8th International Conference on Intelligent Systems: Theories and Applications (SITA)*, Rabat, Morocco, May 2013, pp. 1–8, https://doi.org/10.1109/SITA.2013.6560799.

[10] J. H. Holland, "Genetic Algorithms," *Scientific American*, vol. 267, no. 1, pp. 66–73, 1992.

[11] H. Jafarzadeh, N. Moradinasab, and M. Elyasi, "An Enhanced Genetic Algorithm for the Generalized Traveling Salesman Problem," *Engineering, Technology & Applied Science Research*, vol. 7, no. 6, pp. 2260–2265, Dec. 2017, https://doi.org/10.48084/etasr.1570.

[12] S. Kirkpatrick, C. D. Gelatt, and M. P. Vecchi, "Optimization by Simulated Annealing," *Science*, vol. 220, no. 4598, pp. 671–680, May 1983, https://doi.org/10.1126/science.220.4598.671.

[13] C. Cauchois, E. Brassart, C. Drocourt, and P. Vasseur, "Calibration of the omnidirectional vision sensor: SYCLOP," in *Proceedings 1999 IEEE International Conference on Robotics and Automation (Cat. No.99CH36288C)*, Detroit, MI, USA, 1999, vol. 2, pp. 1287–1292, https://doi.org/10.1109/ROBOT.1999.772538.

[14] M. Abdul-Niby, M. Alameen, A. Salhieh, and A. Radhi, "Improved Genetic and Simulating Annealing Algorithms to Solve the Traveling Salesman Problem Using Constraint Programming," *Engineering, Technology & Applied Science Research*, vol. 6, no. 2, pp. 927–930, Apr. 2016, https://doi.org/10.48084/etasr.627.

[15] S. Fengjie, W. He, and F. Jieqing, "2D Otsu Segmentation Algorithm Based on Simulated Annealing Genetic Algorithm for Iced-Cable Images," in *2009 International Forum on Information Technology and Applications*, Chengdu, China, May 2009, pp. 600–602, https://doi.org/10.1109/IFITA.2009.171.

[16] Y. Chakrapani and K. S. Rajan, "Hybrid Genetic-Simulated Annealing Approach for Fractal Image Compression," *International Journal of Computational Intelligence*, vol. 4, no. 4, pp. 309–314, 2008.

[17] Z. Zhang, "A flexible new technique for camera calibration," *IEEE Transactions on Pattern Analysis and Machine Intelligence*, vol. 22, no. 11, pp. 1330–1334, Aug. 2000, https://doi.org/10.1109/34.888718.

[18] R. Tsai, "A versatile camera calibration technique for high-accuracy 3D machine vision metrology using off-the-shelf TV cameras and lenses," *IEEE Journal on Robotics and Automation*, vol. 3, no. 4, pp. 323–344, Aug. 1987, https://doi.org/10.1109/JRA.1987.1087109.

[19] J. Heikkila and O. Silven, "A four-step camera calibration procedure with implicit image correction," in *Proceedings of IEEE Computer Society Conference on Computer Vision and Pattern Recognition*, San Juan, Puerto Rico, 1997, pp. 1106–1112, https://doi.org/10.1109/CVPR.1997.609468.

[20] Y. Xing, Q. Liu, J. Sun, and L. Hu, "Camera Calibration Based on Improved Genetic Algorithm," in *2007 IEEE International Conference on Automation and Logistics*, Jinan, China, Aug. 2007, pp. 2596–2601, https://doi.org/10.1109/ICAL.2007.4339018.

[21] X. Song, B. Yang, Z. Feng, T. Xu, D. Zhu, and Y. Jiang, "Camera Calibration Based on Particle Swarm Optimization," in *2009 2nd International Congress on Image and Signal Processing*, Tianjin, China, Oct. 2009, pp. 1–5, https://doi.org/10.1109/CISP.2009.5302889.

[22] A. Safaei and S. Fazli, "A novel solution in the simultaneous deep optimization of RGB-D camera calibration parameters using metaheuristic algorithms," *Turkish Journal of Electrical Engineering and Computer Sciences*, vol. 26, no. 2, pp. 743–754, Jan. 2018, https://doi.org/10.3906/elk-1706-250.

[23] S. Ran, L. Ye, J. L. Wang, and Q. Zhang, "A Novel Camera Calibration Method Based on Simulated Annealing Genetic Algorithm," *Applied Mechanics and Materials*, vol. 719–720, pp. 1184–1190, 2015, https://doi.org/10.4028/www.scientific.net/AMM.719-720.1184.

[24] X. Zheng, X. Wang, Z. Luo, and B. Guo, "Camera Imaging Calibration Optimization for Stereo Vision System of Marine Unmanned Ship,"

Journal of Coastal Research, vol. 111, no. SI, pp. 288–292, Dec. 2020, https://doi.org/10.2112/JCR-SI111-052.1.

[25] D. Ge, X. Yao, C. Hu, and Z. Lian, "Nonlinear camera model calibrated by neural network and adaptive genetic-annealing algorithm," *Journal of Intelligent & Fuzzy Systems*, vol. 27, no. 5, pp. 2243–2255, Jan. 2014, https://doi.org/10.3233/IFS-141188.

[26] E. Akbari Sekehravani, E. Babulak, and M. Masoodi, "Implementing canny edge detection algorithm for noisy image," *Bulletin of Electrical Engineering and Informatics*, vol. 9, no. 4, pp. 1404–1410, Aug. 2020, https://doi.org/10.11591/eei.v9i4.1837.